

QUANTITATIVE ASSESSMENT OF TEMPERATURE MITIGATION EFFECT OF RICE PADDY BY NOAA/AVHRR

C.H. Tan^{*}
J.H. Chen^{**}
C.E. Kan^{***}

*Agricultural Engineering Research Center
196-1, ChungYuan Rd., Chung-Li, 320, China Taipei
Tel: (886)3-452-1314 Fax: (886)3-452-6583
E-mail: chtan@aerc.org.tw

**Department of Civil Engineering
National Pingtung University of Science and Technology, China Taipei

***Department of Bioenvironmental Systems Engineering
National China Taipei University, China Taipei

KEY WORDS: Rice Paddy, Temperature Mitigation, NOAA/AVHRR

ABSTRACT

As the economics development and actively trade in the international market, it is inevitable that part of the rice paddy followed or gradually shifted to upland crops in China Taipei. However, the environmental impacts of reduction of rice paddy are complicated for a quantitative assessment. The study use remotely sensed image to evaluate the temperature impact of paddy field reduction. The local surface temperature was derived using the thermal bands of satellite imagery and calibrated with temperature records at weather stations in this study. The unit percentage temperature component for each land use was calculated by solving the multiple equations of random repetitive observation. Results indicated that the unit percentage temperature component of paddy land use was 8.50 °C lower than that of urban land use. The average temperature raised 1.8 °C if 20% of the rice paddy were converted to urban land in the area. The average temperature raised 2.65 °C if there were 30% paddy land converted to urban. According to the results, it is recommended that the government should keep a certain amount of paddy land and limit the number of land development projects in an area, in order to maintain the stability of local environmental temperature.

1. INTRODUCTION

Due to the green house effect and over -development in many places of the world, the climate changed gradually and the frequency of flood inundation and drought increased. Among those phenomenons, the global warming is one of the most significant and extensively discussed. The temperature in urban area, due to high percentage of concrete land pavement and exhausts discharged from automobiles and factories, excess heat from air-conditioning of modern buildings, raised to a uncomfortable degree for people who living in the area.

The cultivation of rice paddy plays an indispensable role in sustaining human life and in maintaining the balance of the entire ecosystem in monsoon Asia. In fact, the paddy is justifiably the most suitable form of agriculture for the soil, weather and other geographical conditions in this area. The cultivation of rice paddy takes large amount of irrigation water, especially during sprouting, transplanting, and nutrient growth periods. The fields of rice paddy keep 3 to 6 centimeter of ponding water on the land surface for most of the growing season. The transpiration of rice plants and evaporation from paddy fields consumes significant amount of heat. As a result, the temperature usually feels cooler in areas surrounded with large paddy fields. The cultivation area of paddy rice decreased from 783,600ha in 1956 to 358,400ha in 1998 in China Taipei. In the mean time, the temperature increased significantly as many agricultural land use developed to urban. However, the actual degree of increase is difficult to demonstrate over an extended area mainly due to the lack of records of regional temperature. The temperature at the meteorological station represents point temperature or, at most, temperature of very limited surrounding area. Since the beginning of thermal remote sensing from satellites, remotely sensed observations of the land surface have provided another source of data for examining the heat characteristics over land surfaces. In this study, the thermal band of NOAA/AVHRR images were used to determine surface temperature, and the idea of unit percentage temperature component for each land use was calculated by solving the multiple equations of random repetitive observation. This method can also be used to calculate probable temperature change in

different land use scenarios.

2. MATERIALS AND METHODOLOGY

2.1 Thermal Remote Sensing

The earth surface can be thought to be a physical system which is periodically excited by the sun and which responds in two ways. First, the earth re-emits, by reflection, a portion of the energy that it receives from the sun, mainly in the visible and near infrared part of the electromagnetic spectrum. This part of the radiation, in principle, is the representation of the surface characteristics of the earth which are useful in determining vegetation varieties and conditions, delineating water body and coast lines, discriminating soil and rock types, etc. Secondly, it receives part of the solar energy and emits directly in the thermal infrared portion of the electromagnetic spectrum. This emitted radiation is strongly related to the surface temperature and the emissivity can be used to infer the energy exchanges in the earth-atmospheric boundary.

All objects with temperatures above absolute zero emit electromagnetic (EM) energy. The magnitude and spectral distribution of this energy can be defined by Planck's equation for a perfect radiator

$$M_{\lambda} = \epsilon B_{\lambda}(T) = \frac{2\pi hc^2}{\lambda^5 \exp\left(\frac{hc}{\lambda kT}\right) - 1} \quad (1)$$

where B_{λ} is Planck's function; M_{λ} is the spectral radiant emission, in $\text{W m}^{-2} \text{ m}^{-1}$; h is Planck's constant, $6.626 \cdot 10^{-34}$ J s; c is the speed of light, $2.99792 \cdot 10^8$ ms^{-1} ; λ is the wavelength, in m; k is the Boltzmann constant, $1.38054 \cdot 10^{-23}$ J K^{-1} ; and T is the temperature in degrees Kelvin. This equation describes the spectral emission of an object per unit area per wavelength. Since natural objects are not perfect blackbodies, the above equation needs to be corrected by multiplying by the emissivity ϵ for different materials. The total radiant emission from a surface at a given temperature can then be determined by integrating M_{λ} with respect to wavelength for all wavelengths and resulted in:

$$M(T) = \int_0^{\infty} \epsilon M_{\lambda} d\lambda = \int_0^{\infty} \frac{2\pi \epsilon hc^2}{\lambda^5} \left[\exp\left(\frac{hc}{\lambda kT}\right) - 1 \right]^{-1} d\lambda = \epsilon \sigma T^4 \quad (2)$$

where M is the radiant emission in Wm^{-2} ; and σ is the Stefan-Boltzmann constant, $5.6697 \cdot 10^{-8} \text{Wm}^{-2}\text{K}^{-4}$.

2.2 NOAA AVHRR Data Calibration and Image Processing

The primary environmental sensor for the NOAA satellite series is the Advanced Very High Resolution Radiometer (AVHRR) which is a five channel scanning radiometer sensing in the visible, near infrared, and thermal infrared window regions. The channel width and features are tabulated in Table 1.

Table 1. The NOAA/AVHRR spectral ranges.

	Channel	Spectral ranges	Description
1	0.58-0.68 μm	visible (red)	
2	0.725-1.05 μm	reflected infrared	
3	3.55-3.92 μm	mid infrared	
4	10.3-11.3 μm	thermal infrared	
5	11.5-12.5 μm	thermal infrared	

The AVHRR is a scanning radiometer, utilizing a rotating scan mirror at a rate of 360 rpm. The instantaneous Field of View (IFOV) for all channels is approximately 1.4 milliradians leading to a resolution at the satellite sub-point of 1.1 km for a nominal altitude of 833 km. The instrument has been designed in such a way that the IFOV of the channels can be made coincident within 0.1 milliradians. This instantaneous field of view was chosen so that the satellite motion along its orbit would cause successive scan lines to be contiguous at the sub-point (Schwalb, 1978).

Based on the cloudlessness, 107 days of NOAA/AVHRR images in 1999 were acquired for this study from the receiving station at the Center for Space and Remote Sensing Research, National Central University, China Taipei. After the radiometric, atmospheric, and geometric correction procedures, radiant temperature were derived for those images. The recorded temperatures at the agro-meteorological stations were used to calibrate the results of surface temperature.

2.3 Repetitive Random Sampling Method

The radiant temperature detected by the sensor of satellite is the temperature of a grouping of surface land uses at the pixel scale. In other words, the temperature derived from NOAA/AVHRR is the mixture of temperature from many land uses within the 1.1 by 1.1 km² area. No matter how small the pixel size is, the value indicated by the pixel is always a blend of the corresponding surface characteristics. Therefore, the satellite-detected temperature at a certain area can be assumed a combination of several temperatures from different land use of the area. Assuming that the relationship of the combination is linear and the temperature detected is independent at each pixel, the relationship can be written as follow:

$$\sum_i \hat{u}_i T_i = T_a \quad (3)$$

where \hat{u}_i is the percentage of land use at the i^{th} region; T_i is the surface temperature for the i^{th} region; and T_a is the average temperature for the whole region.

The study area was in the rice paddy cultivation area in Chia-Nan Plain, located in the southwest China Taipei. A Landsat image in 1999 was also used to classify the land use. Five categories of land use, including paddy rice, upland crops, forest, fish ponds, and urban, were identified in the study area. Many rectangular shaped sub-regions were randomly selected within the study area. The surface temperatures were obtained from the NOAA/AVHRR image and area for each land use in the sub-region was calculated from the classified SPOT image.

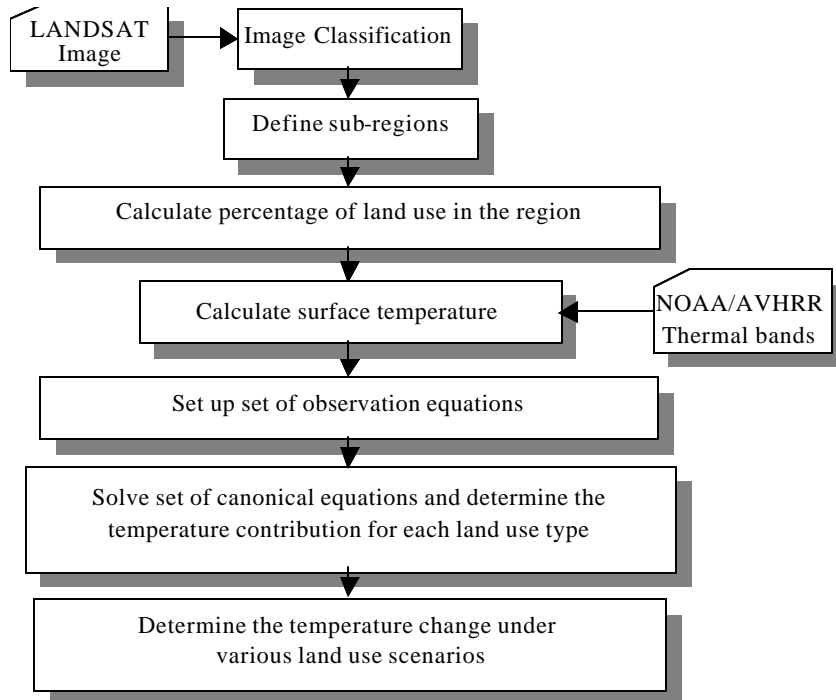
$$\begin{cases} w_{A,1}T_1 + w_{A,2}T_2 + \dots + w_{A,n}T_n = T_A \\ w_{B,1}T_1 + w_{B,2}T_2 + \dots + w_{B,n}T_n = T_B \\ \dots\dots\dots \\ w_{N,1}T_1 + w_{N,2}T_2 + \dots + w_{N,n}T_n = T_N \end{cases} \quad (4)$$

where $\hat{u}_{N,i}$ is the i^{th} land use in the N^{th} sub-region; T_i is the surface temperature for the i^{th} land use sub-region; and T_N is the average temperature for the whole N^{th} region. The number of sub-region N should be greater than the number of land uses. The residual of the observed temperature and the calculated temperature can be defined as:

$$\begin{cases} V_A = w_{A,1}T_1 + w_{A,2}T_2 + \dots + w_{A,n}T_n - T_A \\ V_B = w_{B,1}T_1 + w_{B,2}T_2 + \dots + w_{B,n}T_n - T_B \\ \dots\dots\dots \\ V_N = w_{N,1}T_1 + w_{N,2}T_2 + \dots + w_{N,n}T_n - T_N \end{cases} \quad (5)$$

The surface temperatures for each land use can be determined by minimize the summation of residual squares. The temperatures obtained in the abovementioned equations representing the temperatures contribution from their respective land use. The solution of the abovementioned equation was called the unit percent temperature component T_i (°C/%) for each land use, and those values can be linearly combined with their respect land use percentage within a region. The flow chart for the land use classification and NOAA/AVHRR thermal image, and the determination of temperature component was illustrated in Figure 1.

Figure 1. Flow chart of land classification, thermal band processing and temperature component determination.



3. RESULTS AND DISCUSSIONS

3.1 Land Use Classification

The land use in the ChiaNan study area was divided into six major categories: rice paddy, upland crop (sugarcane), urban, forest, fishpond, and other water bodies. The location, area, emissivity, and corrected surface temperature were listed in table 1.

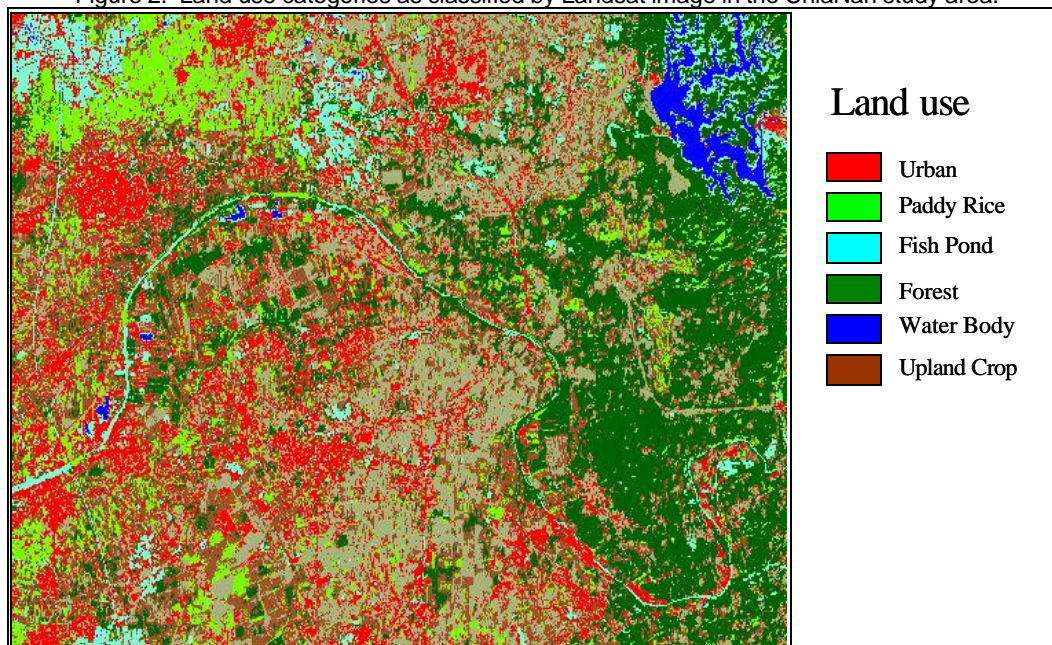
Table 1. Location, area, emissivity, and corrected surface temperature for each land use type.

Land use	Location	Area (km ²)	Emissivity	Elevation (m)	Emissivity corrected temp. (°C)	Elevation corrected temp. (°C)	Station calibrated temp. (°C)
Paddy Rice	YunLin DaBei	10.9	0.98	24.2	30.3	30.5	27.9
	TaiNan LiouJiao	3.2	0.98	6.4	30.5	30.5	27.9
	TaiNan JiaLi	17.4	0.98	4.3	32.6	32.6	29.2
Upland Crop	TaiNan LioFenLiao	5.8	0.96	7.8	35.0	35.0	30.7
	TaiNan BeiShaLun	7.3	0.96	21.7	33.6	33.7	30.0
Urban	ChiaYi City	11.1	0.936	27.5	40.4	40.5	34.2
	TaiNan City	15.1	0.933	22.0	41.3	41.4	34.8
Fish Pond	TaiNan ChiGu	30.1	0.99	2.6	27.9	27.8	26.3
	KaoHsiung HuNei	3.0	0.99	22.0	26.9	27.0	25.7
Forest	Alisan	19.4	0.97	1921.0	15.0	28.4	26.6
	MaTou Mountain	10.5	0.97	574.2	22.0	26.0	25.1

theoretical or area-weighted values.

Land use of the study area was classified by the Landsat image into five land use classes, including urban, paddy rice, upland crop, fish pond, forest, and water body. Figure 2 illustrated the classified image for the study area.

Figure 2. Land use categories as classified by Landsat image in the ChiaNan study area.



A number of rectangular-shaped sub-regions within the ChiaNan study area were randomly selected and set as Area Of Interest (AOI). Figure 3 shows the randomly selected sub-regions with Landsat image in the background. The land use percentage (\hat{u}_i) and average temperature (T_a) in each sub-region were calculated by using the image processing software package ERDAS IMAGINE (Table 2).

Figure 3. Randomly selected sub-regions in the ChiaNan study area.

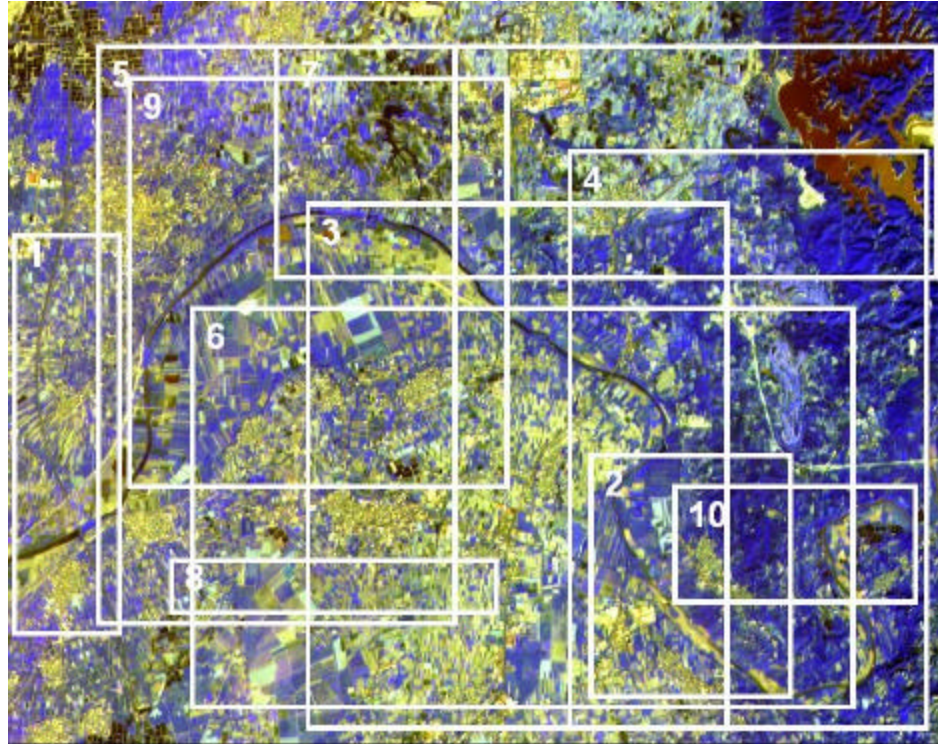


Table 2. Land use percentage (\hat{u}_i) and average temperature (T_a) in each sub-region.

	Urban (%)	Paddy Rice (%)	Fish Pond (%)	Forest (%)	Water Body (%)	Upland Crop (%)	Average Temperature (°C)
Area 1	5.293	25.580	9.923	35.901	9.250	14.052	30.29
Area 2	21.326	33.788	13.910	8.705	0.617	21.654	33.96
Area 3	7.205	23.236	2.530	47.715	0.002	19.312	32.43
Area 4	17.139	29.457	4.421	18.268	0.441	30.275	34.91
Area 5	28.186	21.458	6.794	11.736	0.013	31.814	35.99
Area 6	22.084	39.557	4.542	6.946	0.051	26.820	35.88
Area 7	9.791	29.198	7.382	33.012	3.073	17.543	32.10
Area 8	18.709	37.246	7.237	13.615	0.181	23.011	34.59
Area 9	8.454	28.020	11.238	29.001	10.109	13.179	30.31
Area 10	14.907	30.711	7.342	23.288	1.634	22.118	33.40

The temperature and land use percentage were inputs of a matrix system and created a set of equations as in Equation (4). The canonical equation set can be solved by matrix calculation and the unit percent temperature component T_i (°C/%) of each land use can be obtained. The results were 33.8 °C/% for paddy rice, 28.59 °C/% for forest, 43.30 °C/% for urban, 38.33 °C/% for upland crops, 18.52 °C/% for fish pond, and 19.22 °C/% for other water bodies.

3.2 Surface Temperature with Land Use Scenarios

In order to investigate the environmental temperature impacts induced by land use change, several land use scenarios were adopted to evaluate surface temperature in the ChiaNan area. The average temperature of a 20% land use shift between paddy rice, upland crop, urban, and forest were listed in Table 3.

Table 3. Average temperature and temperature change of several land use change scenarios.

Land use change	Average Temperature (°C)	Temperature Change (°C)
Original Land Use	33.40	
20% paddy rice to upland crop	34.40	1.01
20% paddy rice to urban	35.20	1.80
20% forest to urban	36.24	2.84
20% upland crop to urban	34.29	0.89

The results indicated that the temperature increase slope is 0.9 °C/% in case of paddy rice were developed to urban land use. In other words, the regional temperature increase 2.7 °C in a region with 30% of the paddy field become urban. Other land use scenarios can also be made and the temperature change can be evaluated using the unit percent temperature component method.

5. CONCLUSIONS

The study derived regional temperature using the thermal remote sensing theories and image processing technologies. The local surface temperature was derived using the thermal bands of satellite imagery and calibrated with temperature records at weather stations in this study. The unit percentage temperature component for each land use was calculated by solving the multiple equations of random repetitive observation. Results indicated that the unit percentage temperature component of paddy land use was 8.5 °C lower than that of urban land use. The average temperature raised 1.8 °C if 20% of the rice paddy were converted to urban land in the area. The average temperature raised 2.65 °C if there were 30% paddy land converted to urban. According to the results, it is recommended that the government should keep a certain amount of paddy land and limit the number of land development projects in an area, in order to maintain the stability of local environmental temperature.

6. REFERENCES

- Adams, J. B., M.O. Smith, and A. R. Gillespie, 1989. Simple models for complex natural surfaces: a strategy for the hyperspectral era of remote sensing, Proc. of the IGARSS '89 Symposium, July 10-14, Vol. 1, pp16-21, Vancouver.
- Chen, J. H., 2002. Study on the regional cool effect of rice paddy evapotranspiration. Ph.D. dissertation, National China Taipei University, pp. 187, Taipei. (in Chinese)
- Lillesand, T. M., and R. W. Kiefer, 1987. Remote Sensing and Image Interpretation, 2nd ed. John Wiley and Sons, New York, NY.
- McClain, E. P., W. G. Pichel, and C. C. Walton, 1985. Comparative performance of AVHRR based multi-channel sea surface temperature. Journal of Geophysical Research, 90:11587-11600.
- Ottle, C. and D. Vidal-Madja, 1992. Estimation of Land Surface Temperature with NOAA9 Data, Remote Sensing of Environment, Vol. 40, pp27-41.
- Tan, C. H. and J. H. Chen, 2002. Assessment of Environmental Temperature Affected by Rice Paddy Using Satellite Imagery. Proceedings of the Airborne and Satellite Aided Crop Recognition and Harvest Prediction Conference. pp D1-D8, Taipei, China Taipei.